Ch. 6: Electrochemical Studies

****

This chapter covers the investigations on electrochemical studies of the suitable cathode materials and optimized blend polymer electrolytes in the respectively assembled Ag^+ and Li^+ primary polymer batteries. The chapter mainly undertakes the study of discharge characteristics of these batteries and related battery parameters.

****

6.1 Introduction to Solid State Batteries

The conversion of chemically stored energy into electrical energy through an electrochemical discharge reaction and its storage are of main focus for various practical applications. The major advantage of most of these batteries is that they can be stored for several years in their inactivated and dry state until they are considered for operation [1]. These batteries are basically closed systems of anode and cathode which act as charge-transfer mediums and participate in the redox reactions. In an *'Energy Source'*, anode is a good reducing agent whereas; cathode is an electron acceptor. The reactions at anode usually occur at lower potentials than that at cathode owing to which anode is also termed as 'negative electrode' and indicated as '–' pole and cathode is designated as 'positive electrode' implied by '+' pole.

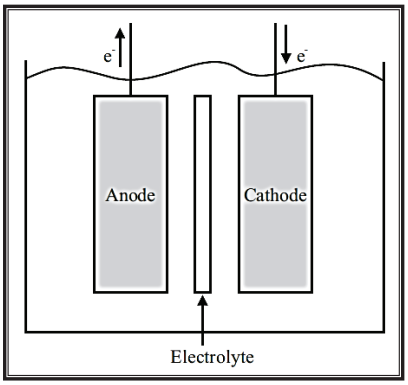

Fig. 6.1 Assembly of a battery/electrochemical cell given as '*Anode*//*Electrolyte*//*Cathode*'

To avoid direct contact of anode and cathode, a porous electrically insulating material containing electrolyte is inserted between anode and cathode. This electrolyte not only physically separates the anode and cathode, but also provides an ionic conduction path for the operation of a battery/electrochemical cell [2]. Most of these batteries are of high energy density and use polymer electrolytes [3,4]. In a solid state battery, all the three components viz. anode, cathode and electrolyte are in solid form. Assembly of such a

battery/electrochemical cell is given as '*Anode* //*Electrolyte* //*Cathode*' and presented in the Fig. 6.1 [5].

♣ ***General Concept of Discharge Characteristics & Operation of a Battery***

Battery operation generally involves conversion of chemical energy to electrical energy through electrochemical discharge reactions. In primary batteries, the reactants once got depleted, cannot be restored again to their fully charged state (as done in secondary batteries by a dc charging source). The depletion reaction in a battery indicates its discharge from a fully charged state and when the reactants get completely depleted, the battery is said to achieve a fully discharged condition. Discharge behaviour of any battery with respect to time further informs about its performance. A profound insight regarding discharge characteristics of any electrochemical battery can be obtained by exploring the behaviour of its current, power or voltage with respect to its discharge time. In ideal case, the voltage remains constant during discharge of a battery followed by its instantaneous drop to zero as soon as the reactants get completely depleted thus, making the battery empty [2,5,6]. Moreover, for all the discharge currents, the ideal capacity of a battery remains constant and the entire energy stored therein, is used completely.

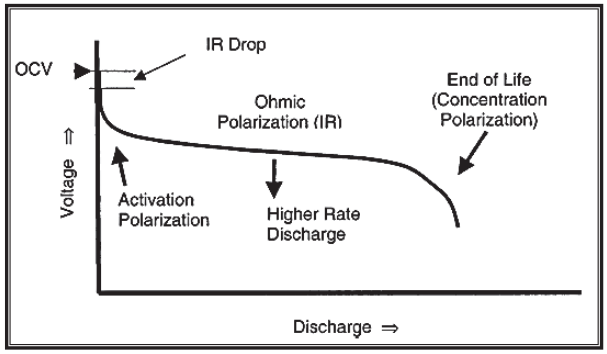

Fig. 6.2 Typical discharge curve of a battery

But in a real practical battery, the voltage slowly drops during the discharge and the effective capacity is low for high discharge currents. A typical discharge curve of a battery is as shown in Fig. 6.2 [2] which directly measures its instantaneous current-voltage

characteristics. Shape of a discharge curve is one of the interesting features wherein, the sloping discharge vs. flat discharge of a battery depends upon its intended usage. A flat, unchanging voltage is preferred for operating a device. On the other hand, for applications wherein, state-of-charge is important, a sloping discharge is preferred [2].

Discharge behaviour of an electrochemical battery can be studied in two major ways one of which includes drawing of a constant current from that battery until its voltage drops to a pre-determined value and another one wherein, the battery is discharged through a constant load (resistance). Out of the two methods the first one tests the battery in reality conditions where a device require to draw a fixed current value which in turn drains a constant current from the battery [6]. There are numerous studies which investigate the discharge behaviour of various batteries with time at different 'C-Rates'. But in the present chapter we study the discharge characteristics of the as assembled Ag^+ and Li^+ primary polymer batteries and their related parameters at different suitable loads of 330 Ω, 1 kΩ, 2.2 kΩ, 3.3 kΩ and 4.7 kΩ that are applied in the external circuit of these batteries.

6.2 Ag^+ Primary Polymer Battery

Silver ion conducting two-phase composite electrolyte systems have received immense importance and attention worldwide owing to their potential use in various electrochemical devices, especially in solid state batteries. It is interesting to inspect the electrochemical performance of 'Ag^+ primary polymer battery'. Hence, in the present battery, '[$PVA_{(50)}$: $PEO_{(50)}$] – 5 wt% $AgNO_3$ – 10 wt% PEG – 6 wt% Al_2O_3' is chosen as an electrolyte in the preparation of such a battery as it depicts optimum ionic transport number and electrical properties as compared to the rest of the blends of Ag^+ conducting series. As in the case of an Ag^+ primary polymer battery, the highly mobile silver ions (Ag^+) dominantly participate in the conduction process, the anode and the cathode have been opted in such a manner that they

promote maximum silver ions (Ag^+) for the conduction process. One of the best fit candidates as anode in the Ag^+ battery is pure Ag metal. Likewise Li, K and Na elements, the silver (Ag) element also offers many beneficial properties such as (i) appreciably high mobility of Ag^+ participating in the conduction process, (ii) highest electrical & thermal conductivity yielding a good capacity value (iii) exceptionally high exchange rates and (iv) economical as compared to other conducting elements. On the other hand, Ag_2O is used as a cathode material in the battery construction by some of the researchers [1,7-10]. **Smith et al.** [7,8] and **Braam et al.** [10] are some of the groups of researchers who contributed in the development of Ag_2O electrode based silver-zinc batteries and observed significantly efficient discharge characteristics of these batteries. On the other hand, **Jayswal et al.** [6], **Guo et al.** [11] and **Padmasree et al.** [12] investigated the performance of the respective silver solid-state batteries prepared using Ag^+ conducting solid electrolytes. Considering this discussion, pure 'Ag' metal is preferred as anode and Ag_2O electrode is selected as cathode in the fabrication of the present Ag^+ primary polymer battery. Discharge characteristics and related parameters of this as prepared Ag^+ primary polymer battery are studied at the various suitable external loads of 330 Ω, 1 kΩ, 2.2 kΩ, 3.3 kΩ and 4.7 kΩ which are applied in its external circuit.

❖ **Discharge Characteristics of Ag^+ Primary Polymer Battery**

At the initial stages, the as prepared 'Ag // $PVA_{(50)}$: $PEO_{(50)}$] − 5 wt% $AgNO_3$ − 10 wt% PEG − 6 wt% Al_2O_3 //Ag_2O' battery is allowed to get stabilized in the open circuit condition (no load connected in external circuit of the battery). The open circuit voltage (OCV) of this battery is obtained to be 0.642 V at discharge time 't = 0' as seen from Fig. 6.3. This OCV value of the present Ag^+ primary polymer battery is found to be considerably closer to the OCV values of the silver based batteries/cells as reported by many workers viz. **Padmasree et al.** [12], **Jayaseelan et al.** [13], **Minami et al.** [14], **Chandra et al.** [15] and **Agrawal et al.** [16,17]. This battery is then subjected to the loads of 330 Ω, 1 kΩ, 2.2 kΩ, 3.3

kΩ and 4.7 kΩ and permitted to undergo a slow and continuous discharge with time. The alteration in the battery voltage vs. discharge time of this battery is depicted in Fig. 6.3. During the discharge process, at each applied load, the battery voltage drops abruptly from OCV with the passing time of the battery discharge. Such a phenomenon is possibly attributed to the active Ohmic polarization of the electrode material and/or the formation of a thin passivating layer of silver (Ag) at the electrode-electrolyte interface.

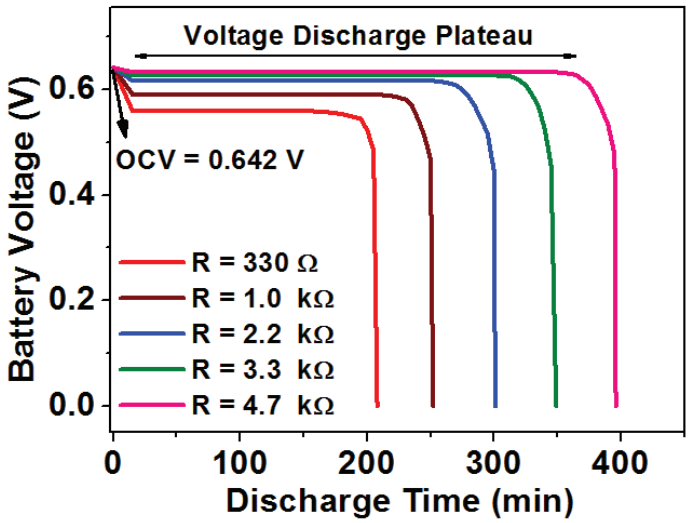

Fig. 6.3 Discharge curve of the as prepared 'Ag^{+} primary polymer battery'

Constant plateau is observed with respect to discharge time till the reactants are available in the battery to carry out the redox reactions. This plateau region is usually termed as the *'Working Region'* of the battery and the voltage corresponding to this plateau region is said to be *'Working Voltage'* or *'Plateau Voltage'*. Finally, at a certain stage (after a certain discharge time) all the reactants are completely used up and hence, the battery gets completely devoid of reactants to avail any further reactions. The complete depletion of reactants directs the battery to the completely discharged state leading to an abrupt drop of the battery voltage to ~ 0 V. But interestingly, as seen from Fig. 6.3, the plateau region starts lasting for longer duration with the addition of loads in the external circuit of the battery, indicating an increase in its discharge time and hence, improvement in its lifetime, as also seen from Table 6.1. Such a phenomenon of the battery is attributed to the gradual reduction

in the current drawn with respect to increase in the loads applied. Additionally, various battery parameters viz. plateau voltage, total discharge time, discharge capacity, specific capacity, electrical energy, specific power and specific energy are calculated at plateau region of the discharge curves at each particular load as shown in the Fig. 6.3. With the addition of loads in the external circuit of the battery, each of these battery parameters improves substantially. However, at each particular load, the specific energy of the battery is considerably much higher than its specific power.

Table 6.1 Battery parameters of 'Ag^+ primary polymer battery' calculated at plateau region

Battery Parameters	***Load = 330 Ω***	***Load = 1 kΩ***	***Load = 2.2 kΩ***	***Load = 3.3 kΩ***	***Load = 4.7 kΩ***
Plateau Voltage (V)	0.561	0.594	0.617	0.628	0.633
Total Discharge Time (min)	208	252	301	347	396
Discharge Capacity (μAh)	1.634	3.205	5.437	9.907	15.292
Specific Capacity (μAh g^{-1})	8.602	16.866	28.614	52.142	80.485
Electrical Energy (μWh)	0.917	1.904	3.354	6.222	9.680
Specific Power (mW kg^{-1})	1.391	2.385	3.517	5.665	7.719
Specific Energy (mWh kg^{-1})	4.826	10.019	17.655	32.745	50.947

6.3 Li^+ Primary Polymer Battery

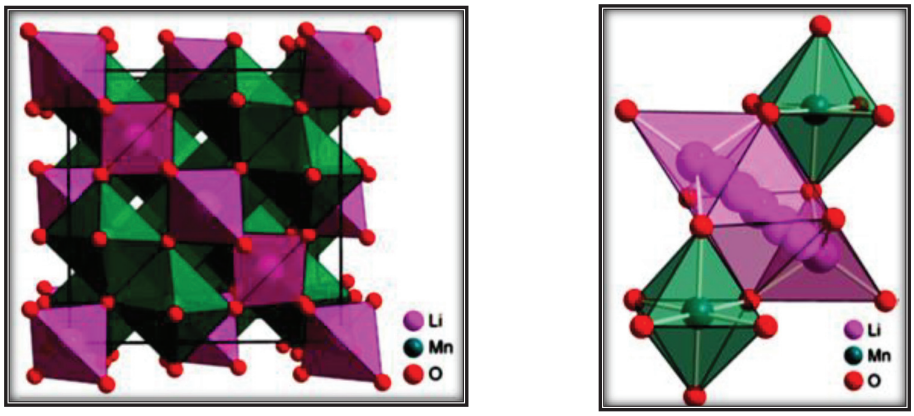

(a) **(b)**

Fig. 6.4 (a) Crystalline spinel structure of $LiMn_2O_4$ cathode
(b) Diffusion of Li^+ through conducting pathways

Lithium based batteries have been identified as most suitable since 1980s for their advanced energy storage capability owing to their superior performance. The performance,

safety and reliability of these Li^+ batteries were further improved after their, commercialization in 1991 by Sony in Japan [18,19]. Though these Li^+ batteries are essential power sources, delivering high energy density since decades, researchers are continuously focussing on further improving their gravimetric energy, power density, safety features, cycling stability and workability in wider temperature range. In the preparation of present Li^+ primary polymer battery, $LiMn_2O_4$ spinel is used as a cathode as it fulfils most of the requirements including low-cost of manganese, high safety, excellent rechargeability, abundance, high working (operating) voltage (~ 4 V), excellent voltage profile characteristics, ease of preparation, satisfactory capacity and high rate performance due to its 3D framework [20-33]. The structure of this $LiMn_2O_4$ cathode is stoichiometric spinel with a cubic unit cell as shown in Fig. 6.4 (a) [34]. $LiMn_2O_4$ basically belongs to AB_2O_4 spinel-type structure consisting of Fd-3m space group symmetry. This structure of $LiMn_2O_4$ basically consists of a close cubic packing arrangement of oxygen (O^{2-}) anions at 32e sites, lithium (Li^+) cations at tetrahedral 8a sites and manganese (Mn^{+3} and Mn^{+4}) cations at octahedral 16d sites. Hence, A, B and O are also designated as tetrahedral and octahedral cation sites and oxygen ion sites, respectively. However, 16c octahedral sites along with 8a tetrahedral sites form 3-dimensional pathways or network of channels ($[Mn_2]O_4$) framework). Insertion and de-insertion of Li^+ in the structure takes place through these vacant octahedral and tetrahedral interstitial spaces of Mn_2O_4 framework i.e. a 3-dimensional tunnel structure viewed as a network of tetrahedral 8a sites. The 3-dimensional network paths through which Li^+ can diffuse during insertion and de-insertion reactions as seen from Fig. 6.4 (b), are given as 8a-16c-8a-16c offered by the lattice [21,33-42]. In such $LiMn_2O_4$ cathode based Li^+ batteries, graphite electrode is often considered as anode. Hence, the present research work deals with the investigation of discharge characteristics of the Li^+ primary polymer battery with graphite electrode as anode along with $LiMn_2O_4$ electrode as cathode. The electrolyte considered in this battery assembly

is '[$PVA_{(50)}$: $PEO_{(50)}$] – 6 wt% EC– 9 wt% $LiCF_3SO_3$ – 10 wt% Al_2O_3' which depicts optimum ionic transport number and electrical properties as compared to the rest of the blend specimens of Li^+ conducting series. The battery is finally assembled in the configuration as 'Graphite // [$PVA_{(50)}$: $PEO_{(50)}$] – 6 wt% EC– 9 wt% $LiCF_3SO_3$ – 10 wt% Al_2O_3 // $LiMn_2O_4$'.

❖ **Discharge Characteristics of Li^+ Primary Polymer Battery**

The as prepared Li^+ primary polymer battery wherein; graphite electrode is considered as anode, $LiMn_2O_4$ electrode as cathode and '[$PVA_{(50)}$: $PEO_{(50)}$] – 6 wt% EC– 9 wt% $LiCF_3SO_3$ – 10 wt% Al_2O_3' as electrolyte is initially equilibrated at open circuit (no load) condition to obtain the open circuit voltage (OCV). OCV value of the as assembled battery is found to be 3.046 V which is slightly lower than the potential values (3.5 V to 4 V) of $LiMn_2O_4$ material [43]. The battery is then allowed to discharge with the passage of time through different loads of 330 Ω, 1 kΩ, 2.2 kΩ, 3.3 kΩ and 4.7 kΩ. It is important to note that as soon as the load is applied to the battery, the battery voltage drops abruptly from OCV of 3.046 V to a certain lower voltage.

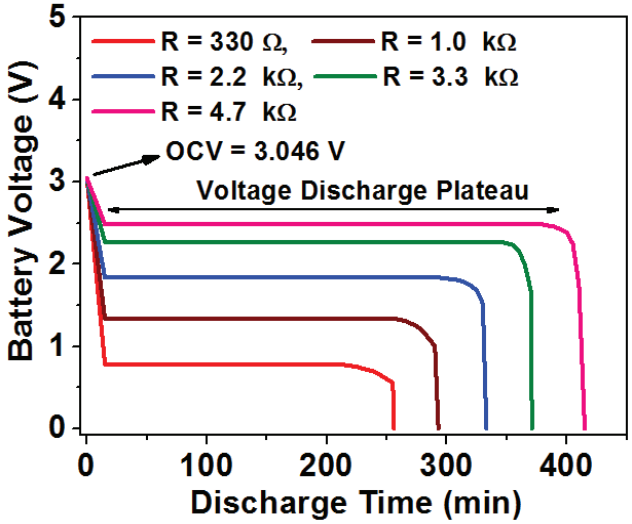

Fig. 6.5 Discharge curve of the as prepared 'Li^+ primary polymer battery'

This phenomenon of abrupt drop of the voltage is observed at each applied load and is due to possible active Ohmic polarization of the electrode material and/or the formation of

thin passivating layer of lithium (Li) at the electrode-electrolyte interface. But at each load condition, after an abrupt drop, the battery voltage becomes constant, yielding a smooth and flat voltage discharge plateau as seen from Fig. 6.5. The region wherein, the battery voltage remains constant with respect to discharge time is termed as *'Plateau Region'* and the voltage corresponding to this plateau region is termed as *'Plateau Voltage'*.

These results are similar to those observed in case of the previously discussed Ag^+ primary polymer battery. This suggests that as the load applied in the external circuit of the battery increases from 330 Ω to 4.7 kΩ, the ability of the present Li^+ primary polymer battery to deliver the amount of electrical energy from its completely charged state to its fully discharged state also increases. Table 6.2 shows the values of discharge capacity as well as specific capacity which continuously increase with the addition of loads. The electrical energy, specific power as well as specific energy of this battery also get significantly enhanced with the increase in loads. This indicates that both power delivering (current drawing) capacity as well as energy delivering capacity of the battery increases with the addition of loads in the battery's circuit.

Table 6.2 Battery parameters of 'Li^+ primary polymer battery' calculated at plateau region

Battery Parameters	***Load = 330 Ω***	***Load = 1 kΩ***	***Load = 2.2 kΩ***	***Load = 3.3 kΩ***	***Load = 4.7 kΩ***
Plateau Voltage (V)	0.788	1.343	1.837	2.274	2.486
Total Discharge Time (min)	256	293	337	371	415
Discharge Capacity (mAh)	2.451	3.919	6.039	9.159	12.636
Specific Capacity (mAh g^{-1})	16.339	26.124	40.257	61.058	84.239
Electrical Energy (mWh)	1.931	5.263	11.093	20.827	31.413
Specific Power (W kg^{-1})	3.015	7.189	14.059	22.467	30.263
Specific Energy (Wh kg^{-1})	12.876	35.085	73.951	138.847	209.419

6.4 Summary

- Various battery parameters including plateau voltage, discharge capacity, specific capacity, electrical energy, specific power and specific energy are calculated at the working region (plateau region) for each applied load in the external circuit of these batteries.
- In both these Ag^+ & Li^+ batteries, all the battery parameters show a significant improvement with the addition of loads from 330 Ω to 4.7 kΩ.
- This suggests that specific energy and specific power of both these Ag^+ & Li^+ batteries enhance with increasing loads.
- All the battery parameters of Li^+ battery are significantly higher than those of Ag^+ at each particular load.
- However, the present Ag^+ and Li^+ primary polymer batteries *'Do Not'* meet the requirements of the commercial Ag^+ & Li^+ primary polymer batteries.
- Hence, the present battery works may be considered as 'preliminary' results only.

References

[1] D.F. Smith, C. Brown, *Journal of Power Sources* 96 (2001) 121.

[2] M. Winter, R.J. Brodd, *Chem. Rev.*104 (2004) 4245.

[3] T.J.R. Reddy, V.B.S. Achari, A.K. Sharma, V.V.R.N. Rao, *Ionics* 13 (2007) 55.

[4] V.M. Mohan, V. Raja, A.K. Sharma, V.V.R.N. Rao, *Ionics* 12 (2006) 219.

[5] M.R. Jongerden, B.R. Haverkort, *Battery Modeling* 1.

[6] M.S. Jayswal, *Ph.D. Thesis*, Department of Physics, The M.S. University of Baroda, 2014.

[7] D.F. Smith, J.A. Gucinski, *Journal of Power Sources* 80 (1999) 66.

[8] D.F. Smith, G.R. Graybill, R.K. Grubbs, J.A. Gucinski, *Journal of Power Sources* 65 (1997) 47.

[9] M. Venkatraman, J.W.V. Zee, *Journal of Power Sources* 166 (2007) 537.

[10] K.T. Braam, S.K. Volkman, V. Subramanian, *Journal of Power Sources* 199 (2012) 367.

[11] Y.G. Guo, Y.S. Hu, J.S. Lee, J. Maier, *Electrochemistry Communications* 8 (2006) 1179.

[12] K.P. Padmasree, D.K. Kanchan, *J. Solid State Electrochem.* 12 (2008) 1561.

[13] S. Jayaseelan, P. Muralidharan, M. Venkateswarlu, N. Satyanarayana, *Materials Science and Engineering B* 119 (2005) 136.

[14] T. Minami, Y. Takuma, M. Tanaka, *J. Electrochem. Soc.* 124 (11) (1977) 1659.

[15] A. Chandra, R.C. Agrawal, Y.K. Mahipal, *J. Phys. D: Appl. Phys.* 42 (2009) 135107.

[16] R.C. Agrawal, R. Ashrafi, D.K. Sahu, Y.K. Mahipal, A. Bhatt, *Indian Journal of Pure & Applied Physics* 51 (2013) 354.

[17] R.C. Agrawal, A. Chandra, A. Bhatt, Y.K. Mahipal, *Eur. Phys. J. Appl. Phys.* 43 (2008) 209.

[18] C.M.I. Bousquet, D.M. Rojas, W.J. Casteel, R.M. Pearlstein, G.G. Kumar, G.P. Pez, M.R. Palacin, *Journal of Power Sources* 195 (2010) 1479.

[19] T. Nagaura, *Prog. Batt. Batt. Mater.* 10 (209) (1991) 218.

[20] M. Michalska, L. Lipinska, M. Mirkowska, M. Aksienionek, R. Diduszko, M. Wasiucionek, *Solid State Ionics* 188 (2011) 160.

[21] M. Aklalouch, R.M. Rojas, J.M. Rojo, I. Saadoune, J.M. Amarill, *Electrochimica Acta* 54 (2009) 7542.

[22] Y. Sun, Z. Wang, X. Huang, L. Chen, *Journal of Power Sources* 132 (2004) 161.

[23] B.J. Hwang, Y.W. Wu, M. Venkateswarlu, M.Y. Cheng, R. Santhanam, *Journal of Power Sources* 193 (2009) 828.

[24] X. Sun, X. Hu, Y.Shi, S. Li, Y. Zhou, *Solid State Ionics* 180 (2009) 377.

[25] S. Mukerjee, X.Q. Yang, X. Sun, S.J. Lee, J. McBreen, Y.E. Eli, *Electrochimica Acta* 49 (2004) 3373.

[26] R. Thirunakaran, A. Sivashanmugam, S. Gopukumar, R. Rajalakshmi, *Journal of Power Sources* 187 (2009) 565.

[27] X. Zhang, H. Zheng, V. Battaglia, R.L. Axelbaum, *Journal of Power Sources* 196 (2011) 3640.

[28] B.J. Kang, J.B. Joo, J.K. Lee, W. Choi, *Journal of Electroanalytical Chemistry* 728 (2014) 34.

[29] Y. Chae, J.K. Lee, W. Choi, *Journal of Electroanalytical Chemistry* 730 (2014) 20.

[30] C.L. Chen, K.F. Chiu, Y.R. Chen, C.C. Chen, H.C. Lin, H.Y. Chiang, *Thin Solid Films* 544 (2013) 182.

[31] C. Peng, H. Bai, M. Xiang, C. Su, G. Liu, J. Guo, *Int. J. Electrochem. Sci.* 9 (2014) 1791.

[32] Q. Liu, S. Wang, H. Tan, Z. Yang, J. Zeng, *Energies* 6 (2013) 1718.

[33] G. Xu, Z. Liu, C. Zhang, G. Cui, L. Chen, *J. Mater. Chem. A* 3 (2015) 4092.

[34] T. Zhang, D. Li, Z. Tao, J. Chen, *Progress in Natural Science: Materials International* 23(3) (2013) 256.

[35] C.M. Julien, A. Mauger, K. Zaghib, H. Groult, *Inorganics* 2 (2014) 132.

[36] F.A. Amaral, N. Bocchi, R.F. Brocenschi, S.R. Biaggio, R.C.R. Filho, *Journal of Power Sources* 195 (2010) 3293.

[37] S. Wang, J. Yang, X. Wu, Y. Li, Z. Gong, W. Wen, M. Lin, J. Yang, Y. Yang, *Journal of Power Sources* 245 (2014) 570.

[38] T. Cui, N. Hua, Y. Han, X. Kang, *Inorganic Materials* 44 (5) (2008) 542.

[39] N. Ishizawa, K. Tateishi, S. Oishi, S. Kishimoto, *American Mineralogist* 99 (2014) 1528.

[40] D. Guo, Z. Chang, B. Li, H. Tang, X.Z. Yuan, H. Wang, *Solid State Ionics* 237 (2013) 34.

[41] D. Arumugam, G.P. Kalaignan, P. Manisankar, *Solid State Ionics* 179 (2008) 580.

[42] B.M. Hwang, S.J. Kim, Y.W. Lee, H.C. Park, D.M. Kim, K.W. Park, *Materials Chemistry and Physics* 158 (2015) 138.

[43] M. Thackarey, *Journal of Chemical Engineering of Japan* 40 (13) (2007) 1150.